The International Society for Optical Engineering

spie.org
spie@spie.org

Mail: PO Box 10
Bellingham, WA
98227-0010 USA

Ship: 1000 20th Street
Bellingham, WA
98225-6705 USA

Tel: +1 360 676 3290
Fax: +1 360 647 1445

-Copyright Statement-

Dear Author,

Publisher's permission is granted to post a copy of your proceedings paper on your, or your company's, website with the stipulation that the following statement is posted on the first page or screen of each paper as posted on the server:

Kind Regards,

Editorial Staff
SPIE Proceedings

*Your manuscript follows this page.

Progress Towards Traceable Nanoscale Optical Critical Dimension Metrology for Semiconductors

Heather J. Patrick[1,2] and Thomas A. Germer[2]

[1]KT Consulting, Inc., Antioch, CA 94509
[2]Optical Technology Division, National Institute of Standards and Technology, Gaithersburg, MD 20899

ABSTRACT

Non-imaging optical critical dimension (OCD) techniques have rapidly become a preferred method for measuring nanoscale features in semiconductors. OCD relies upon the measurement of an optical reflectance signature from a grating target as a function of angle, wavelength and/or polarization. By comparing the signature with theoretical simulations, parameters of the grating lines such as critical dimension (CD) linewidth, sidewall angle, and line height can be obtained. Although the method is sensitive and highly repeatable, there are many issues to be addressed before OCD can be considered a traceable metrology. We report on progress towards accurate, traceable measurement, modeling, and analysis of OCD signatures collected on the NIST goniometric optical scatter instrument (GOSI), focusing on recent results from grating targets fabricated using the single-crystal critical dimension reference materials (SCCDRM) process. While we demonstrate good correlation between linewidth extracted from OCD and that measured by scanning electron microscopy (SEM), we also find systematic deviations between the experimentally obtained optical signatures and best fit theoretical signatures that limit our ability to determine uncertainty in OCD linewidth. We then use the SCCDRM line profile model and a χ^2 goodness-of-fit analysis on simulated signatures to demonstrate the theoretical confidence limits for the grating line parameters in the case of normally distributed noise. This analysis shows that for the current SCCDRM implementation, line height and oxide layer undercut are highly correlated parameters, and that the 3-σ confidence limits in extracted linewidth depend on the target pitch. Prospects for traceable OCD metrology will be discussed.

Keywords: optical critical dimension metrology, scatterometry, semiconductors, rigorous coupled-wave, single-crystal critical dimension reference materials, diffraction, reflectometry, ellipsometry, polarization

1. INTRODUCTION

Semiconductor manufacturing is increasingly done on the nanoscale, requiring measurement techniques that can quickly and non-destructively evaluate features measured in tens of nanometers. Non-imaging optical critical dimension (OCD) techniques are expected to be key technologies in current and future semiconductor manufacutring processes as cited in the most recent version of the International Technology Roadmap for Semiconductors.[1] OCD is a model-based technique in which the characteristics of regular features (such as lines or holes) in a grating target are extracted by comparing a measured optical signature for the target to theoretically generated signatures using a library or regression algorithm.[2,3,4] The optical signature is not an image of the lines in the target, as often the target features are below the diffraction limit, but instead is derived from reflectometry or ellipsometry of all the illuminated lines in the target. In the current work, the optical signatures consist of the reflectance of the grating at a fixed wavelength versus angle of incidence, measured for both s-polarization and p-polarization; a method that is often referred to as angular scatterometry.[2]

Extracting uncertainties and establishing traceability for a scatterometry measurement (or that made by any OCD technique) is complicated by the non-uniqueness of the optical signature to a specific line profile, the nonlinear response of the optical signature to changes in the line profile parameters (such as linewidth, line height, and layer thickness), and the difficulty in identifying systematic errors in the optical signatures. Typically, a priori knowledge of the target line parameters is used to constrain the line profile model used in the generation of theoretical signatures. The line profile model chosen is the simplest structure believed to adequately describe the grating lines, and is necessarily an approximation to the true line structure, making the output parameters dependent on the line profile model chosen. Systematic errors in the collection of the optical signatures are nonlinearly related to changes in the line profile parameters and can be

Advanced Characterization Techniques for Optics, Semiconductors, and Nanotechnologies III, edited by Angela Duparré, Bhanwar Singh, Zu-Han Gu, Proc. of SPIE Vol. 6672, 66720L, (2007) · 0277-786X/07/$18 · doi: 10.1117/12.734080

difficult to characterize and eliminate. Because of this, the disagreement between the theoretical best fit signature and the measured optical signature is often larger than what would be expected using traditional goodness-of-fit metrics.[5]

Despite these difficulties, scatterometry is an extremely useful tool for the characterization of patterned semiconductors. The parameters extracted are usually very repeatable, and the method is sensitive to nanometer-scale changes in groups of similar targets, such as in a process control application. One challenge is to work towards accepted methods for stating and assessing uncertainties in optical signature measurement, in the line profile model, and in the final output parameters.

In this paper, we describe recent work towards the goal of determining uncertainties for OCD scatterometry measurements. We first describe the experimental facility used in our work, the goniometric optical scatter instrument (GOSI), and recent upgrades that enhance our ability to perform scatterometry measurements on grating targets. We then describe modeling capabilities for generation of theoretical optical signatures, and library- and regression-based methods for comparing these signatures with experiment. Next, we summarize recent OCD scatterometry measurements made on grating targets fabricated using the NIST single-crystal critical dimension reference material (SCCDRM) process.[6] This process uses oriented silicon to create lines with vertical sidewalls with widths defined by the silicon lattice plane spacing, and is the basis of an isolated line reference material designed for atomic force microscope (AFM) tip calibrations.[7] We show results for OCD linewidth extracted from scatteromety for a series of SCCDRM grating targets with varying linewidths, and compare to scanning electron microscope (SEM) measurements of the target linewidths. Additionally, the data and theory comparison for these targets is used to demonstrate the sort of systematic variations between theory and experiment often seen in scatterometry. We then turn to the question of the intrinsic sensitivity of the line profile model chosen for the SCCDRM targets to linewidth, line height, and undercuting of the oxide layer. This is done by simulating optical signatures and adding normally distributed noise. The simulated data sets are then fit to the (noiseless) model and a χ^2 goodness-of-fit test used to determine the confidence level in the fitted parameters in the presence of this known noise level. While we stress that this type of uncertainty analysis cannot be applied to the current experimentally measured optical signatures, due to their non-normal noise distribution compared to the theory, the simulated noise method does aid in assessing and predicting the relative uncertainties in extracted line parameters. Finally, we conclude with a summary of progress towards traceable OCD scatterometry and future directions.

2. THE GONIOMETRIC OPTICAL SCATTERING INSTRUMENT (GOSI)

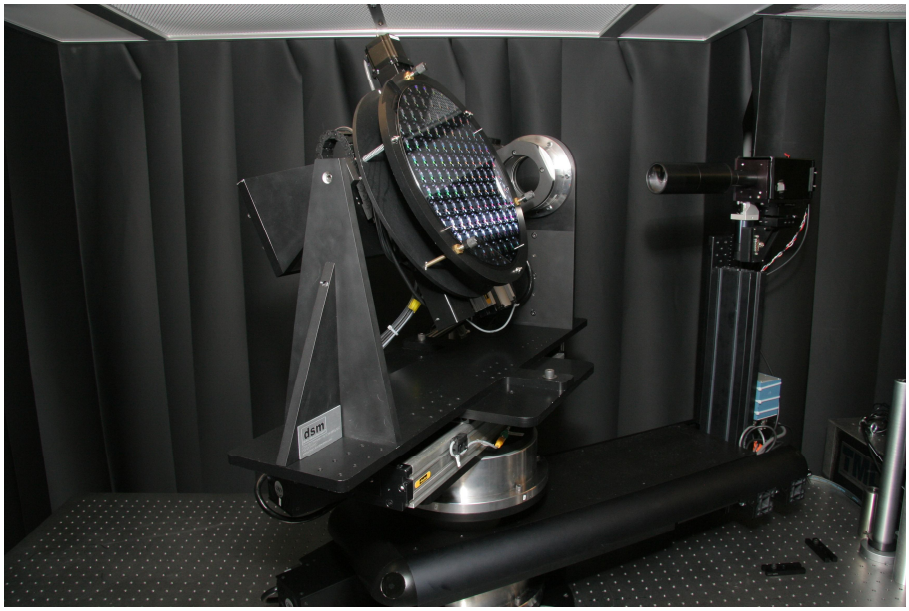

FIG. 1. The goniometric optical scatter instrument (GOSI), with 300 mm wafer on stage and scatterometry detector arm in place.

2.1. GOSI Overview

Figure 1 shows the NIST Goniometric Optical Scatter Instrument (GOSI), with a 300 mm diameter silicon wafer on the sample stage. GOSI is a general-purpose research instrument for making laser-based scattering measurements at wavelengths from 266 nm to 633 nm.[8] In the current work, we use GOSI for angularly resolved scatterometry, making in-plane measurements of the specular reflectance of a grating target for s- and p-polarizations, over a range of angles of incidence. However, the instrument has the flexibility for full hemispherical scattering measurements at nearly any combination of incidence and scattered angles, with multiple detector types providing a wide dynamic range for low light scattering applications. In addition to OCD scatterometry, GOSI applications include nanoscale particle sizing and characterization of surface- and sub-surface roughness of unpatterned samples.[9,10] Recent upgrades have increased the maximum sample size to a 300 mm wafer, achieved micrometer-scale repeatability of target positioning, and extended the operating wavelength to 266 nm UV.

2.2. Scatterometry signature acquisition

The scatterometry measurement setup used in GOSI for this work is shown in Figure 2. Light from a 532 nm laser is incident on a grating target at a variable angle of incidence θ. The light is focused on the target to a roughly gaussian spot with a 20 μm gaussian spot size.[11] The laser polarization is set at either p- (E-field in the plane of incidence) or s- (E-field perpendicular to the plane of incidence) polarization. The detector angle is maintained at twice the angle of incidence (2θ) so that the specular component of the grating reflectance is collected, and θ is varied over a range of 5° to 55°. A small portion of the beam is picked off before the final focusing lens to provide a reference intensity measurement, so that the absolute reflectance (rather than a ratio of s- to p- or similar) can be measured. Figure 4(a) shows example data collected from a grating target for s-polarization (squares) and p-polarization (triangles).

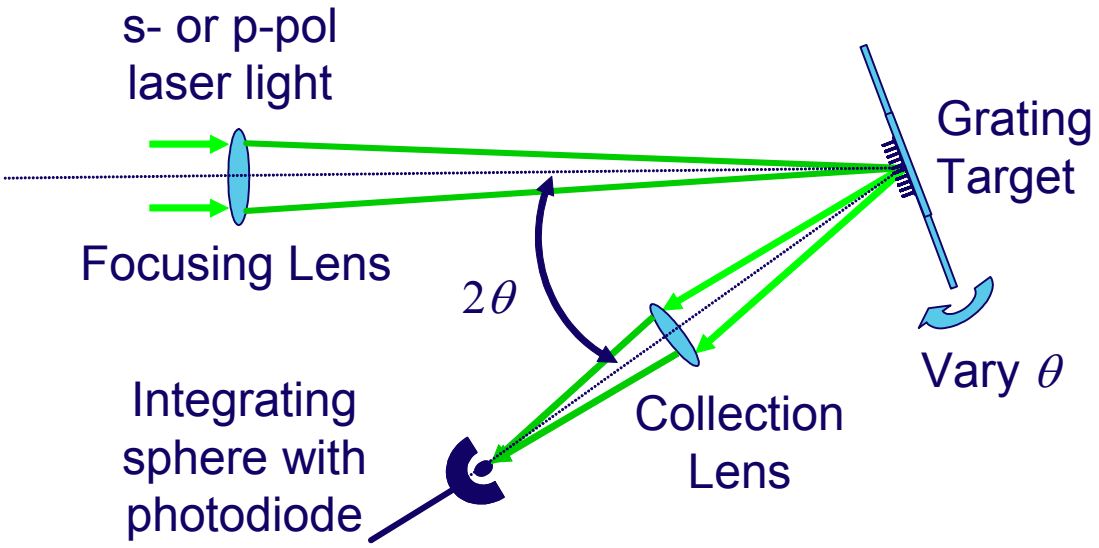

FIG. 2. Orientation of incident beam, target, and detector when collecting specular reflectance scatterometry signatures. The incident laser beam is focused to a roughly 20 μm spot size at the target, and the incident angle is typically scanned over a range of 5° to 55°.

3. MODELING

OCD scatterometry is a model-based measurement method. Optical signatures are collected from a grating target, and a line profile model is developed to describe the parameters of interest in the grating lines, such as linewidth, line height, and layer thicknesses. Theoretical signatures for this line profile model are then generated, and the parameters

that best describe the lines of the target grating are determined by comparing the measured optical signatures with the theoretical signatures. The comparison between theoretical signature and measured signature can be made by generating a library of signatures and searching for the signature that best fits the data (the approach taken here), or can be done using a nonlinear regression algorithm that varies the model parameters to minimize the deviation between theoretical and experimental signatures.[5] The line profile model is generally chosen to be the simplest structure that will adequately describe the lines of the grating and is necessarily an approximation to the actual line shape.

The theoretical optical signatures are obtained using the rigorous coupled wave (RCW) analysis for surface relief gratings developed by Moharam *et al,*,[12,13] with a modification suggested by Lalanne and Morris[14] to improve the convergence of the calculations. This method solves the electromagnetic problem for a plane wave incident upon a medium having a dielectric function $\varepsilon(x,y,z)=\varepsilon_k(x)$, which is periodic in x, independent of y, and independent of z within each of a finite number of layers, indicated by index k. The solution requires Fourier series expansions of $\varepsilon_k(x)$ and $1/\varepsilon_k(x)$ for each layer. In practice, the Fourier series is truncated at some maximum order M; for the SCCDRM targets M was chosen to be 35. The line profile used in modeling the SCCDRM targets is shown in Fig. 3, and has been described in detail previously.[6] The sample consists of a lower silicon substrate with index of refraction n_{Si} = 4.143 + i0.0283[15] an oxide layer of thickness 374 nm with n_{oxide} = 1.462,[15] and between them, a mixed oxide/silicon boundary layer 17 nm thick, which was taken to be a single Bruggeman effective medium layer with a 50/50 mix of oxide and silicon.[16] The grating pitch, p, was taken as known but varied from target to target, while the height, h, and undercut, u were fixed for all the targets at h = 138 nm from reference AFM metrology and u = 8 nm as determined by initial library fitting that took fitting to all targets into account.[6] The OCD linewidth of each target w_{OCD} was then obtained from the measured optical signatures for each target by matching to a library of theoretically generated signatures with varying w. The SCCDRM experimental results for w_{OCD} summarized in Section 4 used fixed h and u determined as described above. In Section 5 we will present a simulated noise study that allows us to examine the effects of also allowing h and u to vary, along with varying w.

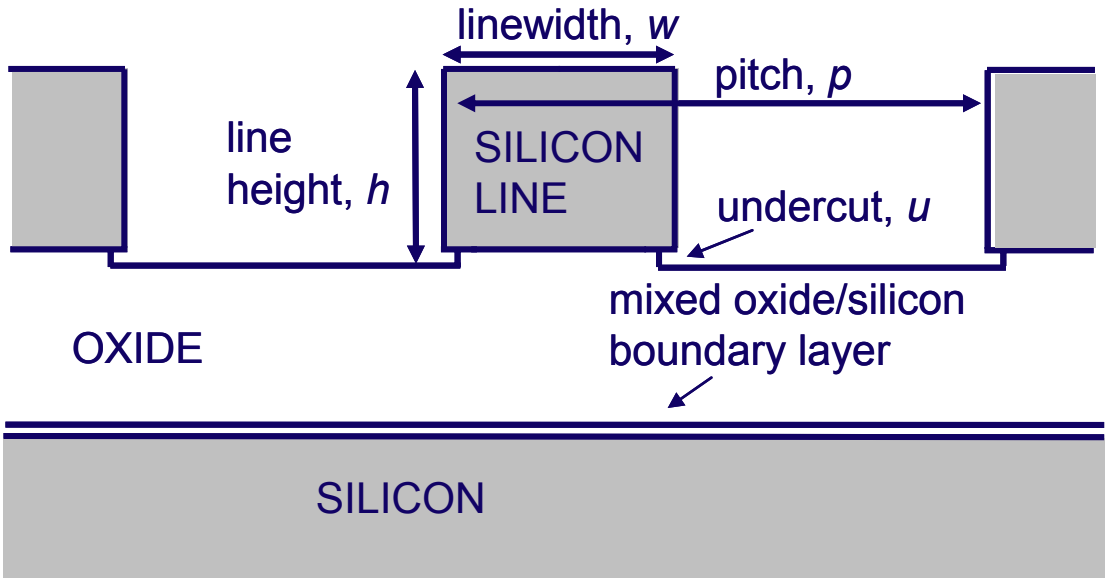

FIG. 3. The line profile model used for RCW modeling of scatterometry signatures of SCCDRM grating targets.

In order to determine the best fit theoretical signature to a given measured optical signature, we minimize the following figure of merit (FOM):

$$\chi_r^2=\frac{1}{(2N-\nu)}\sum_{i=s,p}\sum_{j=1}^{N}\left(\frac{R_{meas,i}(\theta_j)-R_{th,i}(\theta_j)}{\sigma_i(\theta_j)}\right)^2 \qquad (1)$$

where $N = 51$ is the number of discrete angles j where the reflectance is measured, ν is the number of adjustable parameters used when generating the theoretical reflectance signatures, and the subscript i is used to denote that both s- and p-polarization reflectances are included simultaneously when calculating χ^2_r. Inside the summation, $R_{meas,i}(\theta_j)$ is the measured reflectance for the i polarization at the jth angle θ, $R_{ths,i}(\theta_j)$ is the theoretical reflectance for the i polarization at the jth angle θ, and $\sigma_i(\theta_j)$ is the estimated uncertainty in the measured reflectance for the i polarization at the jth angle θ. This equation is the reduced-χ^2 and in principal, for data with normally distributed errors about the best fit theory, can be used to establish confidence limits for the fitted parameters. It will be seen in Section 4, however, that as is common in scatterometry and ellipsometry,[2, 17] our current errors between the data and the modeled signatures are not normally distributed. Nonetheless, for fitting of measured data, we use χ^2_r as a relative measure of goodness-of-fit for different models and different parameter sets. This is identical to an approach that has been taken in analyzing measurements in thin-film ellipsometry.[17] For a specified noise model, we can also use χ^2_r to establish the relative confidence levels for fitting different sets of grating parameters, and this will be shown in Section 5. Similar analysis has recently been used in a study of the theoretical limits to scatterometry sensitivity for different instrumental configurations and process stacks.[18]

4. OCD RESULTS FOR SCCDRM TARGETS

Figure 4 shows the measured and modeled reflectance signatures for a single SCCDRM target (a) and the comparison of target linewidth measured by OCD to that measured by SEM for a series of targets with different design pitches and linewidths (b). The optical signatures shown in Fig. 4(a) are from a target with design pitch of 1400 nm and approximate linewidth (as measured by SEM) of 260 nm. The best fit theory curves for s- and p-polarizations were taken from a library in which the substrate parameters were fixed as described above, the parameters p, u, and h were fixed at p = 1400 nm, u = 8 nm, and h =138 nm, and the width w was varied from 240 nm to 280 nm in 0.5 nm steps. The best fit theoretical curves from this library are shown in Fig. 4(a) and had a value of w = 259.0 nm. In Fig 4(b), we compare the value of w_{OCD} obtained in a similar manner for six SCCDRM grating targets to the value of w_{SEM} measured for each target. We observed good correlation between SEM and OCD measurements, with the slope of w_{OCD} vs. w_{SEM} near unity, with negligible offset.

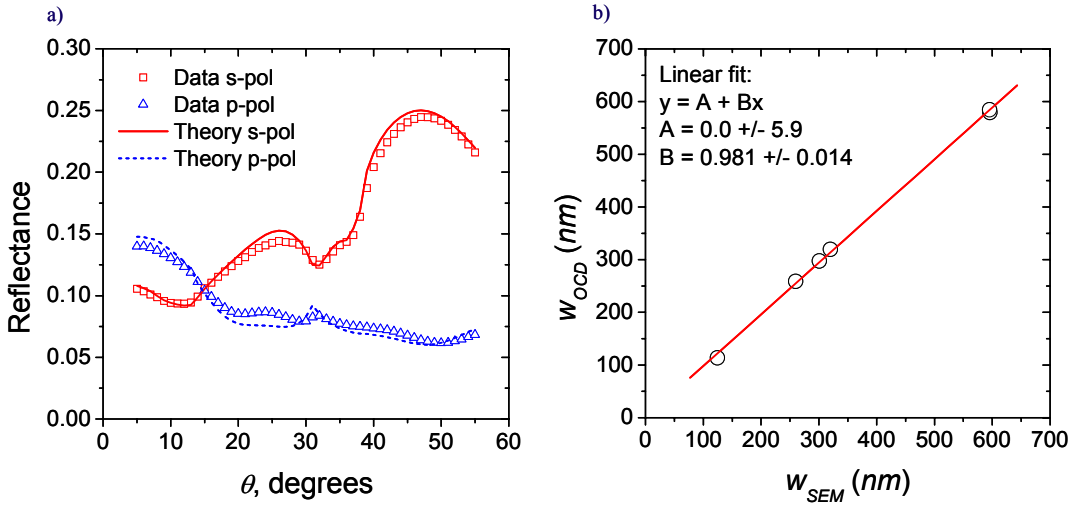

FIG. 4. a) Example of measured s- and p- reflectance spectra (triangles and squares) along with final best fit theory (lines), taken from an SCCDRM target. b) Linewidth extracted using scatterometry OCD (w_{OCD}) versus average linewidth measured across the target using SEM (w_{SEM}), for six different SCCDRM scatterometry targets. Each circle represents the result from an individual scatterometry target.

The repeatability of w_{OCD} on a single target was very good. In previous work, we have shown that the variation in w_{OCD} for repeated measurements of a single target had a standard deviation of only 0.4 nm.[6] However, several difficulties emerge in the fitting of the SCCDRM target signatures to the model. As can be seen in Fig. 4(a), significant residual discrepancies between the data and the model exist, and while the general shape of the measured and theoretical curves

is similar, large sections of data and theory do not overlap. This was seen, to varying degrees, for all of the targets measured and modeled. It was also obvious in the values of χ^2_r for the best fit theoretical signatures. For the library fitting, the value of uncertainty in reflectance $\sigma_i(\theta_j)$ was obtained from the repeatability of the measured reflectance spectra and was estimated as $\sigma_i(\theta_j) = 0.01*R_{meas,i}(\theta_j)$. Using this uncertainty in Eq. (1), the values of χ^2_r ranged from 10 to 138 for the six targets represented in Fig. 4(b). A value of around $\chi^2_r = 1$ is expected for a statistically good fit.[5] While the relatively poor values for χ^2_r could be due in part to underestimation of the random error component of the uncertainty in the measured optical spectra, an additional difficulty is that the differences between theory and data are not randomly distributed. These differences point to systematic errors in the measured optical signatures that may include over-illumination of the target, line edge variations, or other variations of the actual target lines that are not included in the model line profile. The presence of significant systematic errors between data and theory make an objective determination of goodness of fit, and thus the uncertainty in the extracted w_{OCD}, problematic.

While we cannot yet make a complete uncertainty analysis in w_{OCD} due to the presense of systematic errors between the data and the theory, we can use the theory to estimate the predicted parameter sensitivity of SCCDRM targets in different parts of the parameter space (the linewidth sensitivity of targets with similar linewidth but different pitch, for example). We now turn to this analysis.

5. THEORETICAL STUDY OF PARAMETER SENSITIVITY AND UNCERTAINTY

In the case of reflectance datasets with normally distributed noise, goodness-of-fit can be readily evaluated. In analogy with Eq. (1), if the noise at each point in $R_{meas,i}(\theta_j)$ is $\sigma_i(\theta_j)$, then for any theoretically generated reflectance signature $R_{th,i}(\theta_j)$, we can calculate a (non-reduced) χ^2 with respect to the noisy reflectance data, where χ^2 is given by:

$$\chi^2 = \sum_{i=s,p} \sum_{j=1}^{N} \left(\frac{R_{meas,i}(\theta_j) - R_{th,i}(\theta_j)}{\sigma_i(\theta_j)} \right)^2 \tag{2}$$

For the best fit theoretical signature, χ^2 will be at a minimum and χ^2_r [as given by Eq. (1)] will be ≈ 1. However, other theoretical reflectance signatures for other parameter combinations may also have χ^2_r very near 1. The range of values of χ^2 that correspond to "good" fits can be determined from statistics, and this range related to the uncertainty in the fitted parameters. In the case of a library of theoretical signatures as a function of two varied parameters a and b, we plot the set of theoretical signatures with $\Delta\chi^2 \leq 9.0$, where $\Delta\chi^2 = \chi^2(a,b) - \chi^2_{\text{minimum}}$, which forms an ellipse in (a,b) space. The height of the ellipse defines the 3-σ correlated uncertainty for parameter b, while the width of the ellipse is the 3-σ correlated uncertainty for parameter a.[5,19] If more than two parameters are varied in the library, the parameter space becomes multi-dimensional; however, one can still look at the projection of the parameters onto a two-dimensional graph to determine the correlated uncertainty in a parameter.

To illustrate this, we simulated SCCDRM-type reflectance data by calculating a theoretical, noiseless reflectance signature from RCW theory, then adding normally distributed noise with $\sigma_i(\theta_j) = 0.01*R_{noiseless,i}(\theta_j)$. We then fit the simulated noisy signature to a library of theoretical reflectance signatures with a range of SCCDRM line profile parameters, and calculated χ^2 for every parameter combination. Figure 5 shows a plot of all theoretical reflectance signatures that gave a value of $\Delta\chi^2 \leq 9.0$, as a function of the values of h and w of the theoretical signatures. For Fig. 5, the noisy dataset was generated using p = 1400 nm, u = 8 nm, h = 138 nm, and w = 259 nm, with N = 51 angles. The data was fit to a library of models with p and u fixed at the values used for the noisy dataset, but where h and w were varied in 0.01 nm steps. The values of h and w that give good fits to the simulated dataset are seen to be somewhat correlated; the correlated uncertainty region in w, for example is given by the height of the ellipse while it can be seen that if h had been fixed, the uncorrelated uncertainty in w is smaller.

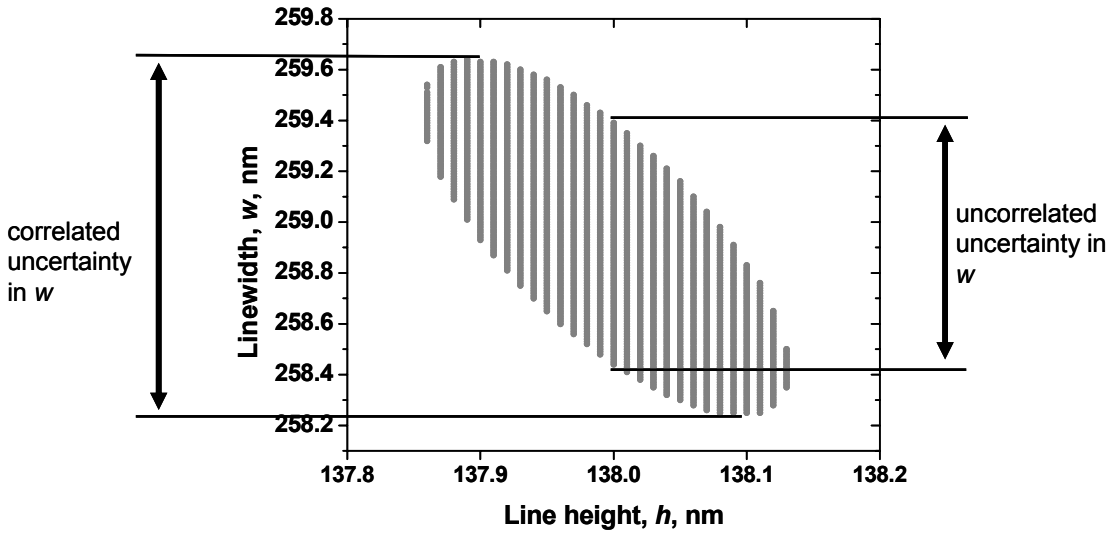

FIG. 5. The 3-σ confidence regions for linewidth, w, and line height h, when linewidth and line height are fitted simultaneously for a simulated noisy dataset, obtained by plotting all combinations of h and w that resulted in a $\Delta\chi^2 \leq 9.0$. Simulated dataset had a nominal parameters w = 259 nm, h = 138 nm, u = 8 nm and p = 1400 nm, with N = 51 angles measured and assuming a reflectance signature noise model of $\sigma = 0.01*R$ as described in the text.

A very interesting observation about the SCCDRM line profile (see Fig. 3) can be seen if instead of varying h and w, h and u are varied. The results of simulating a noisy dataset using p = 2000 nm, w = 579 nm, h = 138 nm, and u = 8 nm, then fitting to a library with fixed p and w, and varying h and u, are shown in Fig. 6. We find a nearly one to one correlation between height and undercut. Other combinations of target parameters (combinations shown in Table 1) gave similar results. This implies that the reflectance spectrum for the SCCDRM line profile is mostly sensitive to the thickness of the silicon line layer, and that extracting the total line height (which includes undercut) from a scatterometry measurement will be hampered by this correlation.

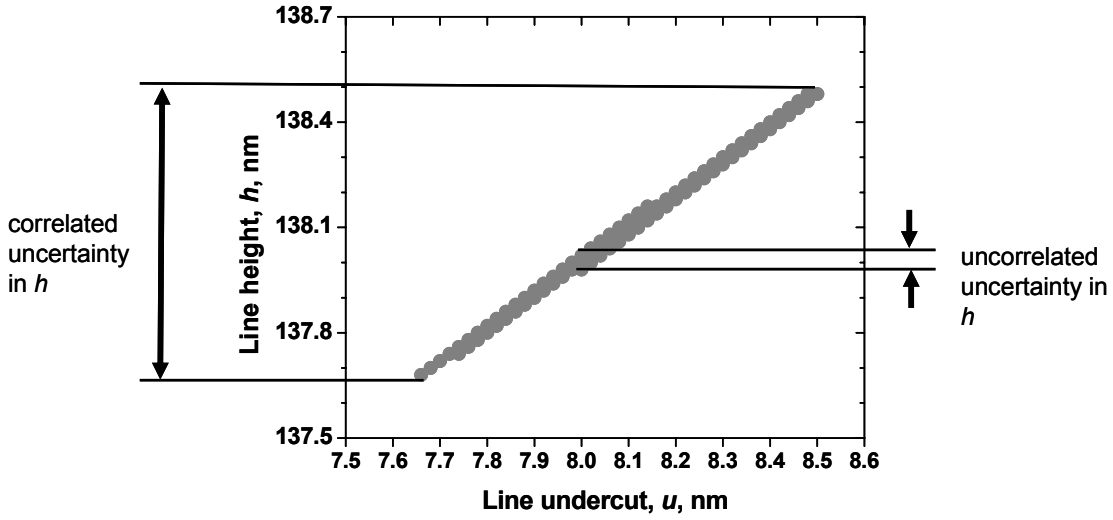

FIG. 6. The 3-σ confidence regions for height, h, and undercut u, when line height and undercut are fitted simultaneously for a simulated noisy dataset, obtained by plotting all combinations of h and w that resulted in $\Delta\chi^2 \leq 9.0$. Simulated dataset had a nominal parameters w = 579 nm, h = 138 nm, u = 8 nm and p = 2000 nm, with N = 51 angles measured and assuming a reflectance signature noise model of $\sigma = 0.01*R$ as described in the text. Similar strong coupling between height and undercut was seen for all the target parameter combinations considered.

Finally, Table 1 demonstrates that the intrinsic sensitivity of scatterometry to linewidth and line height is highly variable over the parameter space of the SCCDRM targets for which we measured w_{OCD} as shown in Section 4. For this table, noisy reflectance datasets with $\sigma_i(\theta_j) = 0.01*R_{noiseless,i}(\theta_j)$ were simulated for each of the target types with parameter combinations shown. Each of these target types corresponds to the approximate values one of the six measured targets represented in Fig. 4(b). Each simulated noisy dataset was then fit to a library with varying h and/or w. The correlated and uncorrelated 3-σ uncertainties are shown in Table 1. Table 1 dramatically illustrates the nonlinear nature of the scatterometry measurement. For example, the extent of the correlated 3-σ confidence ellipse in w for a B1 70s 1:1-type target with w = 259 nm and p = 1400 nm is almost five times that of a B1 70s 1:2-type target with w = 298 nm and p = 3000 nm, even thought the same level of noise on the reflectance signatures was assumed.

	Fixed parameters		Varied parameters and derived uncertainties					
Target Type	p, (nm)	u, (nm)	h, (nm)	w, (nm)	3-σ uncorrelated error in h, (nm)	3-σ uncorrelated error in w, (nm)	3-σ correlated error in h (nm)	3-σ correlated error in w (nm)
B1 00s 1:1	2000	8	138	579	0.04	0.09	0.13	0.3
B1 75s 1:1	1500	8	138	320	0.05	0.13	0.21	0.45
B1 70s 1:1	1400	8	138	259	0.18	0.95	0.27	1.39
B1 00s 1:2	3000	8	138	585	0.08	0.2	0.25	0.57
B1 70s 1:2	2100	8	138	298	0.13	0.14	0.24	0.28
B1 55s 1:2	1650	8	138	114	0.17	0.14	0.85	0.7

TABLE 1. Simulation results for correlated and uncorrelated uncertainty in extracted height h and linewidth w assuming a noise model of σ = 0.01*R as described in the text. There is wide variability in uncertainties despite use of the same noise model for each case. Note these results apply to the simulated random noise case, and should not be taken as the uncertainty estimates for the data shown in Fig. 4(b).

The simulations presented in this section are intended to give a sampling of issues in uncertainty analysis for an idealized case of scatterometry, when the errors in the data are normally distributed about the best fit theoretical simulation. While this does not yet address the problem of systematic errors between data and theory, analysis of the sort shown here can be used to identify how choices of line profile parameters can affect the expected sensitivity to those parameters. We are currently implementing a more flexible and comprehensive modeling capability, OCDSense, that allows us to identifity multiple parameter correlations and also the contributions to uncertainty that are contributed from fixed parameters with a known uncertainty from another reference metrology.

6. SUMMARY AND CONCLUSIONS

We have given an overview of some recent developments in theoretical and experimental capabilities for OCD scatterometry at NIST. Using the measurement of SCCDRM grating targets through scatterometry as an example, we have demonstrated good agreement between linewidth measured by OCD and that measured by SEM, but have also shown the sorts of systematic errors between data and theory that complicate our ability to objectively assess the uncertainties in OCD linewidth. From generating simulated data sets with normally distributed noise, we have assessed the levels of correlated and uncorrelated uncertainties expected for different target parameters. This analysis shows strong correlation of height and undercut, and that the selection of target parameters can dramatically affect the sensitivity of the reflectance signatures to those parameters.

Establishing uncertainties and tracability for OCD scatterometry is an ongoing process. We are continually attempting to understanding and reduce the systematic errors in measurement to the lowest levels possible, to clearly elucidate the line profile models used and their limitations, and to develop and disseminate methods of assessing the theoretical limits of scatterometry sensitivity in the presence of known noise sources. Where appropriate, these activities may involve documentary standards for reporting the results of OCD measurements, artifacts to help identify errors and limitations in OCD data acquisition, and software that can be used for modeling OCD signatures. Through this effort, we

strive to promote a better understanding of OCD measurement and modeling, and to provide tools that enable progress towards OCD tracability.

ACKNOWLEDGEMENTS

We thank the NIST Office of Microelectronics Programs for supporting this work, and acknowledge the use of the NIST Raritan cluster computing system.

REFERENCES

1. http://www.itrs.net/Links/2005ITRS/Metrology2005.pdf
2. C.J. Raymond, M.R. Murnane, S.L. Prins, S.S.H. Naqvi, and J.R. McNeil, "Multiparameter grating metrology using optical scatterometry," J. Vac. Sci. Technol. B, **15**, 361-368 (1997).
3. A. Levy, S. Lakkapragada, W. Mieher, K. Bhatia, U. Whtiney, and M. Hankinson, "Spectroscopic CD Technology for Gate Process Control," *The 2001 IEEE Semiconductor Manufacturing Symposium,* p. 141-144 (2001).
4. W. Yang, J. Hu, R. Lowe-Webb, R. Kohlahalli, D. Shivaprasad, H. Sasano, W. Liu, and D.S.L. Mui, "Line-Profile and Critical-Dimension Monitoring Using a Normal Incidence Optical CD Metrology," IEEE Trans. on Semiconductor Manufacturing, **17**,564-572 (2004).
5. W.H. Press, S.A. Teukolsky, W.T. Vetterling, and B.P. Flannery, *Numerical Recipes in C,* 2nd ed., Cambridge, United Kingdom: Cambridge University Press, 1992.
6. H.J. Patrick, T.A. Germer, M.W. Cresswell, R.A. Allen, R.G. Dixson, and M. Bishop, "Modeling and Analysis of Scatterometry Signatures for Optical Critical Dimension Reference Material Applications," in *Frontiers of Characterization and Metrology for Nanoelectronics 2007*, to be published.
7. M.W. Cresswell, W.F. Guthrie, R.G. Dixson, R.A. Allen, C.E. Murabito, and J.V. Martinez de Pinillos, "RM 8111: Development of a Prototype Linewidth Standard," *J. Res. Of the N.I.S.T.,* **111**, 187-203 (2006).
8. http://physics.nist.gov/lag
9. T.A. Germer and C.C. Asmail, "Polarization of light scattered by microrough surfaces and subsurface defects," J. Opt. Soc. Am. A **18**, 1326-1332 (1999).
10. Germer, T.A., Mulholland, G.W., Kim, J.H., and Ehrman, S.H., "Measurement of the 100 nm NIST SRM® 1963 by laser surface light scattering," in *Advanced Characterization Techniques for Optical, Semiconductor, and Data Storage Components*, A. Duparré and B. Singh, Eds., Proc. SPIE **4779**, 60-71 (2002).
11. A.E. Siegman, *Lasers,* Mill Valley, University Science Books, p. 664, 1986.
12. M.G. Moharam, E.B. Grann, D.A. Pommet, and T.K. Gaylord, "Formulation for stable and efficient implementation of the rigourous couple-wave analysis of binary gratings," J. Opt. Soc. Am. A **12**, 1068-1076 (1995).
13. M.G. Moharam, D.A. Pommet, E.B. Grann, and T.K. Gaylord, "Stable implementation of the rigourous coupled-wave analysis for surface-relief gratings: enhanced transmitance matrix approach," J. Opt. Soc. Am. A **12**, 1077-1086 (1995).
14. P. Lalanne and G.M. Morris, "Highly improved convergence of the coupled-wave method for TM polarization," J. Opt. Soc. Am. A **13**, 779-784 (1996).
15. C.M. Herzinger, B. Johs, W.A. McGahan, J.A. Woolam, and W. Paulson, "Ellipsometric determination of optical constants for silicon and thermally grown silicon dioxide via a multi-sample, multi-wavelength, multi-angle investigation," J. Appl. Phys. **83**, 3323-3336 (1998).
16. H.G. Tompkins, *A User's Guide to Ellipsometry,* New York, Academic, 1993.
17. C.M. Herzinger, P.G. Snyder, B. Johs, and J.A. Woolam, "InP optical constants between 0.75 and 5.0 eV determined by variable-angle spectroscopic ellipsometry," J. Appl. Phys. **77**, 1715-1724 (1995).
18. R. Silver, T. Germer, R. Attota, B.M. Barnes, B. Bunday, J. Allgair, E. Marx and J. Jun, "Fundamental Limits of Optical Critical Dimension Metrology: A Simulation Study," in *Metrology, Inspection, and Process control for Microlithography XXI*, Chas N. Archie, Ed., Proc. SPIE **6518**, 65180U-1 to -17, (2007).
19. G.E. Jellison Jr., "Data analysis for spectroscopic ellipsometry," Thin Solid Films **234**, 416-422 (1993).